HHS Public Access

Author manuscript

J Alzheimers Dis. Author manuscript; available in PMC 2022 January 19.

Published in final edited form as:

J Alzheimers Dis. 2021 ; 81(2): 651–665. doi:10.3233/JAD-201576.

Cortical Thickness, Volume, and Surface Area in the Motoric Cognitive Risk Syndrome

Helena M. Blumen[a,b,*], **Emily Schwartz**[b], **Gilles Allali**[b,c], **Olivier Beauchet**[d], **Michele Callisaya**[e,f], **Takehiko Doi**[g], **Hiroyuki Shimada**[h], **Velandai Srikanth**[e,f], **Joe Verghese**[a,b]

[a]Department of Medicine Albert Einstein College of Medicine, Bronx, NY, USA

[b]Department of Neurology, Albert Einstein College of Medicine, Bronx, NY, USA

[c]Department of Clinical Neurosciences, Geneva University Hospitals and University of Geneva, Switzerland

[d]Division of Geriatric Medicine, Sir Mortimer B. Davis Jewish General Hospital & Dr. Joseph Kaufmann Chair in Geriatric Medicine, Faculty of Medicine McGill University, Montreal, Quebec, Canada

[e]Peninsula Clinical School, Central Clinical School, Monash University, Victoria, Australia

[f]Menzies Institute for Medical Research, University of Tasmania, Tasmania, Australia

[g]Section for Health Promotion, Department of Preventive Gerontology

[h]National Center for Geriatrics and Gerontology, Obu, Aichi, Japan

Abstract

Background: The motoric cognitive risk (MCR) syndrome is a pre-clinical stage of dementia characterized by slow gait and cognitive complaint. Yet, the brain substrates of MCR are not well established.

Objective: To examine cortical thickness, volume, and surface area associated with MCR in the MCR-Neuroimaging Consortium, which harmonizes image processing/analysis of multiple cohorts.

Methods: Two-hundred MRIs (*M* age 72.62 years; 47.74% female; 33.17% MCR) from four different cohorts (50 each) were first processed with FreeSurfer 6.0, and then analyzed using multivariate and univariate general linear models with 1,000 bootstrapped samples (n-1; with resampling). All models adjusted for age, sex, education, white matter lesions, total intracranial volume, and study site.

Results: Overall, cortical thickness was lower in individuals with MCR than in those without MCR. There was a trend in the same direction for cortical volume ($p = 0.051$). Regional cortical thickness was also lower among individuals with MCR than individuals without MCR in prefrontal, insular, temporal, and parietal regions.

[*]Correspondence to: Helena M. Blumen, PhD, Departments of Medicine and Neurology, Albert Einstein College of Medicine, Bronx, NY, 10461 USA. Tel.: +1 718 430 3810; helena.blumen@einsteinmed.org.

Conclusion: Cortical atrophy in MCR is pervasive, and include regions previously associated with human locomotion, but also social, cognitive, affective, and motor functions. Cortical atrophy in MCR is easier to detect in cortical thickness than volume and surface area because thickness is more affected by healthy and pathological aging.

Keywords

Cognitive complaint; cortical thickness; gait; motoric cognitive risk

INTRODUCTION

The motoric cognitive risk (MCR) syndrome is characterized by slow gait and cognitive complaint, and increases the risk for Alzheimer's disease (AD), vascular dementia, and death [1, 2]. Multi-cohort studies of older adults report an MCR prevalence of 9.7%, an MCR incidence of 65.2/1,000 person-years, and the predictive ability of MCR for dementia is greater than either slow gait or cognitive complaint alone [3, 4]. The risk for MCR increases with age, and MCR is more common among older adults with low education, poor social support, depressive symptoms, hypertension, and diabetes, as well as among those who are physically inactive, obese, or have a history of stroke or falls [4–8]. Genetic markers associated with inflammation and obesity are also associated with MCR [9, 10].

We established the MCR-neuroimaging consortium to examine the brain structures and pathologies of MCR in different cohorts. So far, using different subsets of this consortium, we have used voxel-based morphometry and multivariate covariance-based statistics to associate MCR to a pattern of gray matter volume that includes motor, supplementary motor, insular, and prefrontal cortex regions [11]. We have also used manual quantification of lacunes to associate MCR with frontal lacunes [12]. Finally, we have used the age-related white matter changes (ARWMC) scale to show that white matter hyperintensities are not associated with MCR [12–14].

These initial findings suggest that neurodegenerative and some cerebrovascular pathologies, primarily in the cognitive control (or motor planning) pathway of human locomotion, contribute to MCR [15–17] (see Fig. 2). Cognitive (or executive) control processes beyond those needed for human locomotion are also supported by brain regions in this pathway (e.g. prefrontal cortex) and are affected by healthy aging and Alzheimer's disease and related dementias [18–25]. These findings are consistent with and extend a previous observation linking MCR to gray matter in premotor and prefrontal cortex regions [26]. MCR-related atrophy in the cognitive control pathway of human locomotion is also consistent with our recent observation that severity of cognitive impairment (not motoric impairment) predict transition from MCR to dementia [27].

In this study, we examined the relationships between MCR and the cortical thickness, surface area, and volume of different brain regions in the MCR-neuroimaging consortium, using a common image processing pipeline (FreeSurfer) [28, 29]. We hypothesized that cortical atrophy in MCR (less thickness, volume, and surface area in individuals with MCR than those without MCR) would primarily be observed in brain regions that are involved in the control or motor planning aspects of gait, including supplementary motor, insular, and

prefrontal cortex regions. Cortical thickness is typically quantified in millimeters (mm) and reflect the number and/or the complexity (e.g., dendritic branches/spines) of neurons in a column or cortical region [30–32]. Cortical surface area is quantified in squared millimeters (mm^2) and primarily reflect the number of columns in a particular cortical region but can also by influenced by intra-cortical elements such as the volume of the neighboring white matter [32–34]. Finally, cortical volume is quantified in cubic millimeters (mm^3) and is therefore the product of cortical thickness and surface area—and hence reflect a combination of the number or complexity of neurons and columns in a particular cortical region.

Cortical surface area and thickness are both heritable, yet are associated with different genetic and cellular mechanisms, and may therefore be differentially affected in 'healthy' and pathological aging [33, 35, 36]. More specifically, cortical surface area is associated with gene regulation that takes place during early fetal development, cortical thickness is associated with post mid-fetal to adult gene regulation and expression (e.g., neural complexity and myelination), and cortical volume is influenced by a combination of the genetic and cellular mechanisms associated with thickness and surface area. The different genetic and cellular origins of cortical measures likely contribute to that age-related and AD-related cortical changes are easier to detect in cortical thickness than volume and surface area [24, 32, 37–39]. Thus, we further hypothesized that cortical atrophy in MCR would be easier to detect in cortical thickness than volume and surface area.

METHODS

Participants

We examined the data of 200 older adults (*M* Age = 72.62) from 4 different cohorts (50 from each cohort) in the MCR-neuroimaging consortium: 1) the Central Control of Mobility in Aging Study (CCMA; for additional details see [40, 41]) in the US, the Tasmanian Study of Cognition and Gait (TASCOG) [42, 43] in Australia, the Gait and Alzheimer's Interactions Tracking study (GAIT) [26, 44] in France, and the National Center for Geriatrics and Gerontology–Study of Geriatric Syndromes (NCGG-SGS) [45, 46] in Japan. The local institutional review boards at each institution approved all study procedures, and the institutional review board at Albert Einstein College of Medicine approved the consortia analyses presented in this paper. Within each cohort, participants were matched by age and sex. Whenever possible, 25 older adults with MCR and 25 without MCR were selected from each cohort. Some (36.36%) older adults with MCR also had mild cognitive impairment (MCI; see Table 1). Data from one person with corrupted FreeSurfer results were excluded before analyses. Demographic characteristics of the 199 participants that were analyzed are summarized in Table 1. All cohorts, except the GAIT cohort, were recruited directly from the community. GAIT was recruited in a memory clinic.

Outcomes and covariates

MCR was defined as slow gait and cognitive complaint in older adults without dementia and preserved activities of daily living. Individuals with dementia were excluded in all cohorts using the fourth edition of the Diagnostic and Statistical Manual of Mental Disorders (DSM-IV) [47] and a consensus procedure. In the CCMA cohort, MCI status was determined using

DSM-IV and a consensus procedure. In TASCOG, GAIT, and NCGG-SGS, MCI status was defined as cognitive (memory or non-memory) performance 1.5 standard deviation below the mean and presence of cognitive complaint. Gait speed (cm/s) in all cohorts, except NCGG-SGS, was quantified over 20 feet (609.6 cm) with GAITRite instrumented walkways (GAITRite System ® Clifton, NJ). Gait speed in NCGG-SGS was quantified over 240 cm with the WalkWay MW-1000 instrumented walkway (Anima Co., Tokyo, Japan). Slow gait was defined as gait speed more than one standard deviation or more below age and sex-specific means in each cohort, based on previously established procedures [3, 4]. Subjective cognitive complaint was obtained from the Geriatric Depression Scale (GDS) [48] and/or the Ascertain Dementia 8-item Informant Questionnaire [49] in CCMA, from the GDS and/or Instrumental Activities of Daily Living (I-ADL) in TASCOG and NCGG-SGS, and from self-report in GAIT.

Age, sex, education, total intracranial volume, white matter lesions, and study site were covariates. Although previous studies suggest that white matter lesions are not associated with MCR using the manual/semi-quantitative ARWMC scale [12–14], we included the overall white matter lesions measure automatically computed by FreeSurfer as a covariate in our statistical models. This is because we wanted to determine if the associations we observed between MCR and cortical thickness, volume, and surface area went above and beyond those previously observed between white matter lesions and cortical atrophy in aging [50, 51]. This is also because white matter lesions have presumed vascular origins, and MCR is associated with vascular disease and risk factors. Note, however, that because fluid-attenuated inversion recovery (FLAIR) MRIs were not available in all cohorts, overall white matter lesions were estimated from T1-weighted MRIs, and therefore likely underestimates overall white matter lesions burden.

Image acquisition

Images were acquired at each study site, and then transferred to Albert Einstein College of Medicine (Bronx, NY) for centralized/harmonized processing. Images were acquired with a Philips 3T MRI scanner (Achieva Quasar TX; Philips Medical Systems, Best, Netherlands) in CCMA, a General Electric (GE) 1.5 T MRI scanner (GE LX Horizon, Milwaukee, WI) in TASCOG, a Siemens 1.5T MRI scanner (Magnetom Avanto; Siemens Medical Solutions, Erlangen, Germany) in GAIT, and a Siemens 3T MRI scanner (TIM Trio, Siemens, Germany) in NCGG-SGS. Standard three-dimensional T1-weighted images were obtained from all cohorts: 1) CCMA: TR/TE of 9.9/4.6 ms, 240 mm^2 FOV, and 1 mm voxel size (for additional details, see [41]), 2) TASCOG: TR/TE of 37/7 ms, 240 mm^2 FOV, and 1 mm voxel size [42], 3) GAIT: TR/TE 2170/4.07 ms, 240 mm^2 mm FOV, and 1 mm voxel size [26], and 4) NCGG-SGS: TR/TE of 1.98/1800 ms and 1.1 mm voxel size [45].

Image processing

Harmonized (or centralized) image processing was performed at Albert Einstein College of Medicine by the same person (E.S.) on the same computer using the same processing pipeline; FreeSurfer version 6.0: http://surfer.nmr.mgh.harvard.edu/ [28, 29]. FreeSurfer automatically reconstructs cortical regions based on the morphology of the gyri and sulci in each individual, and involves skull stripping, bias field correction, gray-white matter

segmentation, reconstruction of cortical surface, and non-linear registration. Note that while FreeSurfer's fully automated cortical parcellation procedures is comparable to manual labeling [52], it is generally recommended that results are manually inspected and corrected when necessary. Manual error correction methods, however, vary widely across studies and raters, can be quite time-consuming, and may not alter the relationship between cortical measures and cognitive outcomes [53, 54]. Thus, to avoid inter-rater variability and provide us with the opportunity to examine if manual error correction influenced the relationship between cortical measures and MCR, manual error correction was completed by the same individual (E.S.) who was blinded to MCR status and involved using FreeView visualization tools to inspect gray matter and cerebrospinal fluid boundaries on a slice-by-slice basis. Manual error correction included white matter voxel addition or removal, adding white matter control points, and pial or skull removal (see Fig. 1). The FreeSurfer pipeline was then repeated until satisfactory results were obtained for each participant. Mean cortical thickness, volume, and surface area of 34 cortical regions in each hemisphere was then obtained using the Desikan-Killiany atlas [55], and subsequently collapsed (or added) across hemispheres—because we had no hemisphere-specific analyses and wanted to reduce the number of statistical models to be completed.

Statistical approach

Group differences in age, sex, education, white matter lesions, and study site as a function of MCR were first examined with student *t*-test, Mann-Whitney U test, Kruskal-Wallis test, or chi-square tests as appropriate after variables were inspected for potential violations to normality and other statistical assumptions. Two multivariate general linear models (GLM) with 34 brain regions as outcomes were then completed for each cortical measure separately (thickness, volume, and surface area); one for uncorrected mean values, and one for manually corrected mean values. Each multivariate GLM was followed by 34 univariate GLMs for each brain region. Univariate GLMs were only interpreted if the overall multivariate model was significant ($p < 0.05$) and univariate results remained significant after a false discovery rate (FDR) correction for multiple comparisons [56, 57]. To generate more precise estimates of the 95% confidence interval for each univariate model, the reliability of each model was further evaluated using 1,000 randomly generated bootstrapped samples (n-1, with resampling). Bootstrapping methods has been shown to not only generate more precise confidence intervals and error estimates than standard methods, but they also protect against potential violations of the normality assumption of GLMs in accordance with the central limit theorem [58]. The predictor of interest was MCR, and all models were adjusted for age, sex, education, total intracranial volume, white matter lesions, and study site. Analyses were completed with STATA version 14.2 (StataCorp LP, College Station, TX, USA).

RESULTS

The demographic characteristics of the 199 eligible participants are summarized in Table 1. The mean age was 72.62 years, 47.74% female, and 41.71% had 9–12 years of education. The prevalence of MCR (33.17%) was higher than in previous reports [3, 5] due to our sampling strategy. Relative to individuals without MCR, individuals with MCR were

younger (Student t (197) = 3.73, $p < 0.001$) and differed in terms of education quartile (Pearson χ^2 (2) = 14.78. $p < 0.01$) but did not differ in terms of sex (Pearson χ^2 (1) = 0.21, $p = 0.21$) or white matter lesions (Mann-Whitney $z = -0.82$ $p = 0.42$). Twenty-four participants (36.36%) with MCR had MCI. Age (Kruskal Wallis χ^2 (3) = 125.59, $p < 0.001$), education quartile (Pearson χ^2 (6) = 79.38, $p < 0.001$), and white matter lesions (Kruskal Wallis $\chi 2$ (3) = 28.56, $p < 0.001$) differed between cohorts, and cohorts were marginally different in terms of sex (Pearson $\chi 2$ (3) = 6.99 $p = 0.07$).

Cortical thickness

Table 2 summarizes the results of our multivariate and univariate GLMs. Our multivariate models were significant for both uncorrected [$F(340; 1508) = 4.52$, $p < 0.0001$] and corrected [$F(340; 1508) = 4.47$, $p < 0.0001$] cortical thickness. Both cortical thickness models also showed a main effect of MCR [uncorrected: Wilks' lambda (Λ) = 0.744, $p = 0.037$; corrected: $b = 0.730$, $p = 0.019$], age [uncorrected: $\Lambda = 0.614$, $p < 0.0001$; corrected: $\Lambda = 0.663$, $p < 0.0001$], education [uncorrected: $\Lambda = 0.536$, $p = 0.002$; corrected: $\Lambda = 0.571$, $p = 0.017$], white matter lesions [uncorrected: $\Lambda = 0.745$, $p = 0.038$; corrected: $\Lambda = 0.688$, $p = 0.002$], and study site [uncorrected: $\Lambda = 0.036$, $p < 0.0001$; corrected: $\Lambda = 0.037$, $p < 0.0001$], but no main effect of sex [uncorrected: $\Lambda = 0.781$, $p = 0.164$; corrected $\Lambda = 0.780$, $p = 0.161$] or total intracranial volume [uncorrected: $\Lambda = 0.775$, $p = 0.136$; corrected $\Lambda = 0.830$, $p = 0.588$]. Follow-up univariate models revealed that uncorrected and corrected cortical thickness were significantly lower among older adults with MCR than those without MCR in prefrontal, insular, temporal and parietal regions—including entorhinal [uncorrected 95% CI = −0.508; −0.107; corrected 95% CI = −0.510; −0.106], inferior parietal [uncorrected 95% CI = −0.258; −0.052; corrected 95% CI = −0.251; −0.055], lateral orbitofrontal [uncorrected 95% CI = −0.273; −0.031; corrected 95% CI = −0.262; −0.033], medial orbitofrontal [uncorrected 95% CI = −0.286; −0.042; corrected 95% CI = −0.312; −0.067], parstriangularis [uncorrected 95% CI = −0.284; −0.113; corrected 95% CI = −0.272; −0.089], and insular [uncorrected 95% CI = −0.291; −0.065; corrected 95% CI = −0.278; −0.068] regions (see Table 2). While uncorrected cortical thickness was lower among individuals with MCR than those without MCR in isthmus cingulate, pars orbitalis, and posterior cingulate regions, they did not survive the FDR adjustment in manually corrected cortical thicknesses. Moreover, while manually corrected cortical thickness was lower among older adults with MCR in the superior temporal region, it did not survive the FDR adjustment for uncorrected cortical thickness. Despite these minor discrepancies in significance between regional uncorrected and corrected mean cortical thickness, the 95% confidence intervals for all 34 regions overlapped (see Table 2)—indicating that the estimated relationships between cortical thickness and MCR did not significantly differ following manual correction.

Cortical volume

Our multivariate models were significant for both uncorrected [$F(340; 1508) = 3.52$, $p < 0.0001$] and corrected [$F(340; 1508) = 3.52$, $p < 0.0001$] cortical volume. Like cortical thickness models, both cortical volume models revealed significant main effects of age [uncorrected: $\Lambda = 0.708$, $p = 0.006$; corrected: $\Lambda = 0.650$, $p < 0.001$], white matter lesions [uncorrected: $\Lambda = 0.637$, $p < 0.0001$; corrected: $\Lambda = 0.668$, $p < 0.001$] and

study site [uncorrected: $\Lambda = 0.148$, $p < 0.0001$; corrected: $\Lambda = 0.160$, $p < 0.0001$]. Both cortical volume models, however, showed only a marginally significant main effect of MCR [uncorrected: $\Lambda = 0.751$, $p = 0.051$; corrected: $\Lambda = 0.763$, $p = 0.084$], and a main effect of total intracranial volume [uncorrected: $\Lambda = 0.391$, $p < 0.0001$; corrected: $\Lambda = 0.391$, $p < 0.0001$]. The main effect of education was not significant in the uncorrected or corrected models [uncorrected: $\Lambda = 0.681$, $p = 0.566$; corrected: $\Lambda = 0.665$, $p = 0.443$]. Finally, there was no main effect of sex in the uncorrected model [uncorrected: $\Lambda = 0.770$, $p = 0.113$], but there was a main effect of sex in the corrected model [corrected: $\Lambda = 0.746$, $p = 0.041$]. Given that the main effect of MCR was only marginally significant in our multivariate models, we will not describe the results of the follow-up univariate models (see Table 2) beyond that the 95% confidence intervals for all 34 regions overlapped—indicating that the estimated relationships between cortical volume and MCR did not significantly differ following manual correction.

Cortical surface area

Our multivariate models were significant for both uncorrected [$F(340; 1508) = 3.42$, $p < 0.0001$] and corrected [$F(340; 1508) = 3.47$, $p < 0.0001$] cortical surface area. In both surface area models, there was a main effect sex [uncorrected: $\Lambda = 0.717$, $p = 0.009$; corrected: $\Lambda = 0.711$, $p = 0.007$], white matter lesions [uncorrected: $\Lambda = 0.636$, $p < 0.0001$; corrected: $\Lambda = 0.665$, $p < 0.001$], total intracranial volume [uncorrected: $\Lambda = 0.401$, $p < 0.0001$; corrected: $\Lambda = 0.388$, $p < 0.0001$], and study site [uncorrected: $\Lambda = 0.143$, $p < 0.0001$; corrected: $\Lambda = 0.135$, $p < 0.0001$]. In both surface area models, however, there was no main effect of MCR [uncorrected: $\Lambda = 0.774$, $p = 0.130$; corrected: $\Lambda = 0.757$, $p = 0.066$] or education level [uncorrected: $\Lambda = 0.697$, $p = 0.706$; corrected: $\Lambda = 0.690$, $p = 0.646$]. The main effect of age was significant for uncorrected cortical surface [uncorrected: $\Lambda = 0.739$, $p = 0.029$] and marginally significant for corrected cortical surface [uncorrected: $\Lambda = 0.754$, $p = 0.059$]. Since there was nomain effect of MCR on cortical surface areas in our multivariate models, we will not describe the results of our follow-up univariate models (see Table 2) further than that the 95% confidence intervals for all 34 regions overlapped—indicating that the estimated relationships between cortical surface area and MCR did not change following manual correction.

DISCUSSION

This study examined the relationships between cortical thickness, volume and surface area and a pre-clinical stage of dementia called the motor cognitive risk syndrome, with a common image-processing pipeline (Free Surfer). Our key findings are that 1) MCR was associated with a widespread pattern of cortical atrophy that included prefrontal, insular and parietal regions (see Table 2), 2) cortical thickness was more sensitive to cortical atrophy in MCR than volume and surface area, and 3) manual correction did not alter the relationships between MCR, cortical thickness, volume, and surface area.

Cortical atrophy in MCR is widespread

As hypothesized, a widespread pattern of cortical atrophy was associated with MCR. Cortical atrophy was observed in regions that are part of the control pathway of human

locomotion such as prefrontal, insular and parietal regions (Table 2) [16, 59]. These regions are also associated with a number of social, cognitive, and affective functions. The prefrontal cortex, for example, is primarily associated with executive functions, and particularly affected in aging [20, 60–63]. The medial prefrontal cortex has been specifically linked to social cognition [62, 63] and the insula is not only associated with drives and emotions, but also attention and memory awareness [60, 64]. Cortical atrophy in MCR was also observed in the entorhinal cortex (a medial temporal lobe regions that is important for learning and memory), which is affected by MCI and is a reliable predictor of the conversion from MCI to AD [65, 66]. These results are consistent and extend our previous studies [11, 26]. Taken together, it is clear that cortical atrophy in MCR is pervasive, and involve regions not only associated with human locomotion, but also social, cognitive and affective functions - which is consistent with previous findings that MCR is associated with social [8], cognitive [1, 3, 4] and affective [4] outcomes and risk factors.

Cortical atrophy in MCR is easier to detect in cortical thickness than volume or surface area

As hypothesized, cortical thickness was significantly lower in individuals with MCR than in individuals without MCR. Yet, cortical volume and surface area were not significantly associated with MCR (although trends were observed in the expected direction). These findings are consistent with that cortical thickness and cortical surface area are attributed to different genetic and cellular mechanisms, and that cortical volume likely is attributed to a combination of both mechanisms [33, 35, 36]. These findings are also consistent with that cortical thickness is more sensitive to age-related and AD-related cortical changes than cortical volume or cortical surface areas [24, 32, 39]. Note also that the volumetric changes that are observed in aging have been primarily attributed to thickness rather than surface area [24]. Thus, the cortical atrophy we observed in MCR here likely are more attributed to neuronal number and complexity loss rather than the combination of neuronal number, neuronal complexity, and column loss. To our knowledge, this is the first time that cortical thickness has been examined in the context of MCR and contrasted with other cortical measures.

Manual intervention did not alter the relationships between cortical measures and MCR

As hypothesized, the estimated relationships between MCR and cortical thickness, volume, and surface area were not significantly altered when manual correction of the cortical surface was a component of our image-processing pipeline. This finding is consistent with a previous study that found that the relationships between cortical measures and cognitive performance does not change following error correction [53]. We observed this finding even though inter-rater variability was eliminated by having the same person (E.S.) complete the error correction procedure, a feat that is difficult to accomplish in larger data sets or consortiums. In such situations, careful development of error checking manuals or procedures can reduce inter-rater variability, but the process remains both time and labor intensive. The findings of the current study suggest that error correction may not be necessary when examining the relationship between cortical measures in the MCR-neuroimaging consortium.

Strength and weaknesses

There are a number of notable strengths and weaknesses of this study. Pooling data and resources from four different cohorts allowed us to quickly and efficiently examine the relationships between different cortical measures and MCR. Variability unrelated to the relationships of interest were reduced by 1) using a harmonized image processing pipeline, 2) adjusting for key confounders (age, sex, education, total intracranial volume, and study site) and other major contributors to age-related cortical atrophy (white matter lesions), and 3) employing a sensitive (multivariate) statistical approach that permitted us to formally assess the reliability of our findings (bootstrap). Inter-rater reliability for the manual component of our image-processing pipeline was further eliminated by having one person complete the error correction procedure. This approach afforded us the ability to link a pervasive pattern of cortical atrophy to MCR that included regions previously associated with human locomotion, and social, cognitive, and affective functions. This approach also allowed us to show that cortical atrophy in MCR may be easier to detect in cortical thickness than cortical volume and surface area—and that the relationship between MCR and different cortical measures does not change following manual intervention.

Despite concerted efforts to reduce unwanted variability, pooling data and resources from different cohorts introduces variability that is difficult to adjust for with any statistical approach, particularly when sample size is limited. Future studies using a larger subset of the MCR-neuroimaging consortium will determine the reliability of these findings and permit us to consider other potential confounders and interactions. A more precise measure of overall white matter lesion burden, for example, may provide a more precise picture of the association between MCR and cortical atrophy (recall that our estimates came from T1-weighted images because FLAIR images were not available in all cohorts, and therefore likely underestimates overall white matter lesion burden). It is also important to note that while cortical thickness has good reliability across measures and study sites (intra-class correlation coefficients > 0.80), cortical thickness has been shown to be less reliable across studies than cortical volume using an earlier version of the FreeSurfer 6.0 software used in this study (version 5.1) [67, 68]. Again, future studies using FreeSurfer and other imaging pipelines (e.g., CAT12 [69], are needed to confirm the reliability of these cross-sectional findings. Longitudinal studies are also needed to examine changes in cortical thickness, volume and surface area in individuals with MCR.

CONCLUSION

Establishing the brain substrates of MCR provides insights into the pathogenesis of MCR and provides the foundation for future biological and intervention studies. Given that MCR has been associated with some vascular pathologies in the past [12], and is associated with cortical atrophy in regions previously linked to human locomotion as well as social, cognitive, and affective functions in the current study—multi-modal interventions that are socially, carodiovascularly, and cognitively demanding (e.g., social dancing) may be a promising avenue of intervention.

ACKNOWLEDGMENTS

This study was supported by NIH/NIA grants: 1R56AG057548-01 and R01AG057548-01A1.

Authors' disclosures available online (https://www.j-alz.com/manuscript-disclosures/20-1576r1).

REFERENCES

[1]. Verghese J, Wang C, Lipton RB, Holtzer R (2012) Motoric cognitive risk syndrome and the risk of dementia. J Gerontol A Biol Sci Med Sci 68, 412–418. [PubMed: 22987797]

[2]. Ayers E, Verghese J (2016) Motoric cognitive risk syndrome and risk of mortality in older adults. Alzheimers Dement 12, 556–564. [PubMed: 26545790]

[3]. Verghese J, Annweiler C, Ayers E, Barzilai N, Beauchet O, Bennett DA, Bridenbaugh SA, Buchman AS, Callisaya ML, Camicioli R (2014) Motoric cognitive risk syndrome Multicountry prevalence and dementia risk. Neurology 83, 718–726. [PubMed: 25031288]

[4]. Verghese J, Ayers E, Barzilai N, Bennett DA, Buchman AS, Aron S, Holtzer R, Katz M, Lipton RB, Wang C (2014) Motoric cognitive risk syndrome: Multicenter incidence study. Neurology 83, 2278–2284. [PubMed: 25361778]

[5]. Callisaya ML, Ayers E, Barzilai N, Ferrucci L, Guralnik JM, Lipton RB, Otahal P, Srikanth VK, Verghese J (2016) Motoric cognitive risk syndrome and falls risk: A multicenter study. J Alzheimers Dis 53, 1043–1052. [PubMed: 27340851]

[6]. Doi T, Verghese J, Shimada H, Makizako H, Tsutsumimoto K, Hotta R, Nakakubo S, Suzuki T (2015) Motoric cognitive risk syndrome: Prevalence and risk factors in Japanese seniors. J Am Med Dir Assoc 16, 1103. e1121–1103. e1125.

[7]. Beauchet O, Sekhon H, Barden J, Liu-Ambrose T, Chester VL, Szturm T, Grenier S, Léonard G, Bherer L, Allali G, Canadian Gait C (2018) Association of motoric cognitive risk syndrome with cardiovascular disease and risk factors: Results from an original study and meta-analysis. J Alzheimers Dis 64, 875–887. [PubMed: 29966199]

[8]. Felix N, Ayers E, Verghese J, Blumen HM (2020) Association of the motoric cognitive risk syndrome with levels of perceived social support. Alzheimers Dement 16(7 Suppl), e039489.

[9]. Sathyan S, Barzilai N, Atzmon G, Milman S, Ayers E, Verghese J (2017) Association of anti-inflammatory cytokine IL10 polymorphisms with motoric cognitive risk syndrome in an Ashkenazi Jewish population. Neurobiol Aging 58, 238.e1–238.e8.

[10]. Sathyan S, Wang T, Ayers E, Verghese J (2019) Genetic basis of motoric cognitive risk syndrome in the Health and Retirement Study. Neurology 92, e1427–e1434. [PubMed: 30737336]

[11]. Blumen HM, Allali G, Beauchet O, Lipton RB, Verghese J (2018)A gray matter volume covariance network associated with the motoric cognitive risk syndrome: A multi-cohort MRI study. J Gerontol A Biol Sci Med Sci 74, 884–889.

[12]. Wang N, Allali G, Kesavadas C, Noone ML, Pradeep VG, Blumen HM, Verghese J (2016) Cerebral small vessel disease and motoric cognitive risk syndrome: Results from the Kerala-Einstein study. J Alzheimers Dis 50, 699–707. [PubMed: 26757037]

[13]. Mergeche J, Verghese J, Allali G, Wang C, Beauchet O, Kumar V, Mathuranath P, Yuan J, Blumen H (2016) White matter hyperintensities in older adults and motoric cognitive risk syndrome. J Neuroimaging Psychiatry Neurol 1, 73–78. [PubMed: 28630950]

[14]. Wahlund L-O, Barkhof F, Fazekas F, Bronge L, Augustin M, Sjögren M, Wallin A, Adèr H, Leys D, Pantoni L (2001) A new rating scale for age-related white matter changes applicable to MRI and CT. Stroke 32, 1318–1322. [PubMed: 11387493]

[15]. la Fougere C, Zwergal A, Rominger A, Forster S, Fesl G, Dieterich M, Brandt T, Strupp M, Bartenstein P, Jahn K (2010) Real versus imagined locomotion: A [18F]-FDG PET-fMRI comparison. Neuroimage 50, 1589–1598. [PubMed: 20034578]

[16]. Zwergal A, Linn J, Xiong G, Brandt T, Strupp M, Jahn K (2012) Aging of human supraspinal locomotor and postural control in fMRI. Neurobiol Aging 33, 1073–1084. [PubMed: 21051105]

[17]. Leisman G, Moustafa AA, Shafir T (2016) Thinking, walking, talking: Integratory motor and cognitive brain function. Front Public Health 4, 94. [PubMed: 27252937]

[18]. Elderkin-Thompson V, Ballmaier M, Hellemann G, Pham D, Kumar A (2008) Executive function and MRI prefrontal volumes among healthy older adults. Neuropsychology 22, 626–637. [PubMed: 18763882]

[19]. West RL (1996) An application of prefrontal cortex function theory to cognitive aging. Psychol Bull 120, 272–292. [PubMed: 8831298]

[20]. Raz N, Gunning FM, Head D, Dupuis JH, McQuain J, Briggs SD, Loken WJ, Thornton AE, Acker JD (1997) Selective aging of the human cerebral cortex observed *in vivo*: Differential vulnerability of the prefrontal gray matter. Cereb Cortex 7, 268–282. [PubMed: 9143446]

[21]. Raz N (2000) Aging of the brain and its impact on cognitive performance: Integration of structural and functional findings In The handbook of aging and cognition (2nd ed.), Craik FIM, Salthouse TA, eds. Lawrence Erlbaum Associates Publishers, Mahwah, NJ, US, pp. 1–90.

[22]. Driscoll I, Davatzikos C, An Y, Wu X, Shen D, Kraut M, Resnick S (2009) Longitudinal pattern of regional brain volume change differentiates normal aging from MCI. Neurology 72, 1906–1913. [PubMed: 19487648]

[23]. Salat DH, Buckner RL, Snyder AZ, Greve DN, Desikan RS, Busa E, Morris JC, Dale AM, Fischl B (2004) Thinning of the cerebral cortex in aging. Cerebr Cortex 14, 721–730.

[24]. Storsve AB, Fjell AM, Tamnes CK, Westlye LT, Overbye K, Aasland HW, Walhovd KB (2014) Differential longitudinal changes in cortical thickness, surface area and volume across the adult life span: Regions of accelerating and decelerating change. J Neurosci 34, 8488–8498. [PubMed: 24948804]

[25]. Kennedy KM, Rodrigue KM, Bischof GN, Hebrank AC, Reuter-Lorenz PA, Park DC (2015) Age trajectories of functional activation under conditions of low and high processing demands: An adult lifespan fMRI study of the aging brain. Neuroimage 104, 21–34. [PubMed: 25284304]

[26]. Beauchet O, Allali G, Annweiler C, Verghese J (2016) Association of motoric cognitive risk syndrome with brain volumes: Results from the GAIT study. J Gerontol A Biol Sci Med Sci 71, 1081–1088. [PubMed: 26946101]

[27]. Verghese J, Wang C, Bennett DA, Lipton RB, Katz MJ, Ayers E (2019) Motoric cognitive risk syndrome and predictors of transition to dementia: A multicenter study. Alzheimers Dement 15, 870–877. [PubMed: 31164315]

[28]. Fischl B, Sereno MI, Dale AM (1999) Cortical surface-based analysis: II: Inflation, flattening, and a surface-based coordinate system. Neuroimage 9, 195–207. [PubMed: 9931269]

[29]. Dale AM, Fischl B, Sereno MI (1999) Cortical surface-based analysis: I. Segmentation and surface reconstruction. Neuroimage 9, 179–194. [PubMed: 9931268]

[30]. Peters A, Morrison J, Rosene DL, Hyman BT (1998) Are neurons lost from the primate cerebral cortex during normal aging? Cereb Cortex 8, 295–300. [PubMed: 9651126]

[31]. Freeman SH, Kandel R, Cruz L, Rozkalne A, Newell K, Frosch MP, Hedley-Whyte ET, Locascio JJ, Lipsitz LA, Hyman BT (2008) Preservation of neuronal number despite age-related cortical brain atrophy in elderly subjects without Alzheimer disease. J Neuropathol Exp Neurol 67, 1205–1212. [PubMed: 19018241]

[32]. Lemaitre H, Goldman AL, Sambataro F, Verchinski BA, Meyer-Lindenberg A, Weinberger DR, Mattay VS (2012) Normal age-related brain morphometric changes: Nonuniformity across cortical thickness, surface area and gray matter volume? Neurobiol Aging 33, 617.e611–617.e619.

[33]. Winkler AM, Kochunov P, Blangero J, Almasy L, Zilles K, Fox PT, Duggirala R, Glahn DC (2010) Cortical thickness or grey matter volume? The importance of selecting the phenotype for imaging genetics studies. Neuroimage 53, 1135–1146. [PubMed: 20006715]

[34]. Feczko E, Augustinack JC, Fischl B, Dickerson BC (2009) An MRI-based method for measuring volume, thickness and surface area of entorhinal, perirhinal, and posterior parahippocampal cortex. Neurobiol Aging 30, 420–431. [PubMed: 17850926]

[35]. Panizzon MS, Fennema-Notestine C, Eyler LT, Jernigan TL, Prom-Wormley E, Neale M, Jacobson K, Lyons MJ, Grant MD, Franz CE (2009) Distinct genetic influences on cortical surface area and cortical thickness. Cereb Cortex 19, 2728-2735. [PubMed: 19299253]

[36]. Grasby KL, Jahanshad N, Painter JN, Colodro-Conde L, Bralten J, Hibar DP, Lind PA, Pizzagalli F, Ching CRK, McMahon MAB, et al. (202) The genetic architecture of the human cerebral cortex. Science 367, eaay6690. [PubMed: 32193296]

[37]. Hutton C, Draganski B, Ashburner J, Weiskopf N (2009) A comparison between voxel-based cortical thickness and voxel-based morphometry in normal aging. Neuroimage 48, 371–380. [PubMed: 19559801]

[38]. Dickerson BC, Feczko E, Augustinack JC, Pacheco J, Morris JC, Fischl B, Buckner RL (2009) Differential effects of aging and Alzheimer's disease on medial temporal lobe cortical thickness and surface area. Neurobiol Aging 30, 432–440. [PubMed: 17869384]

[39]. Schwarz CG, Gunter JL, Wiste HJ, Przybelski SA, Weigand SD, Ward CP, Senjem ML, Vemuri P, Murray ME, Dickson DW (2016) A large-scale comparison of cortical thickness and volume methods for measuring Alzheimer's disease severity. Neuroimage Clin 11, 802–812. [PubMed: 28050342]

[40]. Holtzer R, Mahoney J, Verghese J (2014) Intraindividual variability in executive functions but not speed ofprocessing or conflict resolution predicts performance differences in gait speed in older adults. J Gerontol A Biol Sci Med Sci 69, 980–986. [PubMed: 24285744]

[41]. Blumen HM, Holtzer R, Brown LL, Gazes Y, Verghese J (2014) Behavioral and neural correlates of imagined walking and walking while talking in the elderly. Hum Brain Mapp 35,4090–4104. [PubMed: 24522972]

[42]. Callisaya ML, Beare R, Phan TG, Chen J, Srikanth VK (2014) Global and regional associations of smaller cerebral gray and white matter volumes with gait in older people. PLoS One 9, e84909. [PubMed: 24416309]

[43]. Srikanth V, Phan TG, Chen J, Beare R, Stapleton JM, Reutens DC (2010) The location of white matter lesions and gait–a voxel-based study. Ann Neurol 67, 265–269. [PubMed: 20225293]

[44]. Beauchet O, Allali G, Launay C, Herrmann F, Annweiler C (2013) Gait variability at fast-pace walking speed: A biomarker of mild cognitive impairment? J Nutr Health Aging 17, 235–239. [PubMed: 23459976]

[45]. Doi T, Blumen HM, Verghese J, Shimada H, Makizako H, Tsutsumimoto K, Hotta R, Nakakubo S, Suzuki T (2017) Gray matter volume and dual-task gait performance in mild cognitive impairment. Brain Imaging Behav 11, 887–898. [PubMed: 27392792]

[46]. Shimada H, Tsutsumimoto K, Lee S, Doi T, Makizako H, Lee S, Harada K, Hotta R, Bae S, Nakakubo S (2016) Driving continuity in cognitively impaired older drivers. Geriatr Gerontol Int 16, 508–514. [PubMed: 25953032]

[47]. American Psychiatric Association (1994) Diagnostic and Statistical Manual of Mental Disorders, American Psychiatric Association.

[48]. Yesavage JA, Brink TL, Rose TL, Lum O, Huang V, Adey M, Leirer VO (1982) Development and validation of a geriatric depression screening scale: A preliminary report. J Psychiatr Res 17, 37–49. [PubMed: 7183759]

[49]. Galvin JE, Roe CM, Powlishta KK, Coats MA, Muich SJ, Grant E, Miller JP, Storandt M, Morris JC (2005) The AD8: A brief informant interview to detect dementia. Neurology 65, 559–564. [PubMed: 16116116]

[50]. Habes M, Erus G, Toledo JB, Zhang T, Bryan N, Launer LJ, Rosseel Y, Janowitz D, Doshi J, Van der Auwera S, von Sarnowski B, Hegenscheid K, Hosten N, Homuth G, Völzke H, Schminke U, Hoffmann W, Grabe HJ, Davatzikos C (2016) White matter hyperintensities and imaging patterns of brain ageing in the general population. Brain 139, 1164–1179. [PubMed: 26912649]

[51]. Wen W, Sachdev PS, Chen X, Anstey K (2006) Gray matter reduction is correlated with white matter hyperintensity volume: A voxel-based morphometric study in a large epidemiological sample. Neuroimage 29, 1031–1039. [PubMed: 16253521]

[52]. Fischl B, van der Kouwe A, Destrieux C, Halgren E, Ségonne F, Salat DH, Busa E, Seidman LJ, Goldstein J, Kennedy D, Caviness V, Makris N, Rosen B, Dale AM (2004) Automatically parcellating the human cerebral cortex. Cereb Cortex 14, 11–22. [PubMed: 14654453]

[53]. Waters AB, Mace RA, Sawyer KS, Gansler DA (2019) Identifying errors in Freesurfer automated skull stripping and the incremental utility of manual intervention. Brain Imaging Behav 13, 1281–1291. [PubMed: 30145718]

[54]. McCarthy CS, Ramprashad A, Thompson C, Botti J-A, Coman IL, Kates WR (2015) A comparison of FreeSurfer-generated data with and without manual intervention. Front Neurosci 9, 379. [PubMed: 26539075]

[55]. Desikan RS, Ségonne F, Fischl B, Quinn BT, Dickerson BC, Blacker D, Buckner RL, Dale AM, Maguire RP, Hyman BT (2006) An automated labeling system for subdividing the human cerebral cortex on MRI scans into gyral based regions of interest. Neuroimage 31, 968–980. [PubMed: 16530430]

[56]. Benjamini Y, Hochberg Y (1995) Controlling the false discovery rate: A practical and powerful approach to multiple testing. J R Stat Soc Series B Methodol 57, 289–300.

[57]. Glickman ME, Rao SR, Schultz MR (2014) False discovery rate control is a recommended alternative to Bonferroni-type adjustments in health studies. J Clin Epidemiol 67, 850–857. [PubMed: 24831050]

[58]. Efron B, Tibshirani R (1986) Bootstrap methods for standard errors, confidence intervals, and other measures of statistical accuracy. Statist Sci 1, 54–75.

[59]. Rosso AL, Studenski SA, Chen WG, Aizenstein HJ, Alexander NB, Bennett DA, Black SE, Camicioli R, Carlson MC, Ferrucci L, Guralnik JM, Hausdorff JM, Kaye J, Launer LJ, Lipsitz LA, Verghese J, Rosano C (2013) Aging, the central nervous system, and mobility. J Gerontol A Biol Sci Med Sci 68, 1379–1386. [PubMed: 23843270]

[60]. Menon V, Uddin LQ (2010) Saliency, switching, attention and control: A network model of insula function. Brain Struct Funct 214, 655–667. [PubMed: 20512370]

[61]. Uddin LQ, Nomi JS, Hébert-Seropian B, Ghaziri J, Boucher O (2017) Structure and function of the human insula. J Clin Neurophysiol 34, 300–306. [PubMed: 28644199]

[62]. Bzdok D, Langner R, Schilbach L, Engemann DA, Laird AR, Fox PT, Eickhoff S (2013) Segregation of the human medial prefrontal cortex in social cognition. Front Hum Neurosci 7, 232. [PubMed: 23755001]

[63]. Gutchess AH, Kensinger EA, Schacter DL (2007) Aging, self-referencing, and medial prefrontal cortex. Soc Neurosci 2, 117–133. [PubMed: 18633811]

[64]. Cosentino S, Brickman AM, Griffith E, Habeck C, Cines S, Farrell M, Shaked D, Huey ED, Briner T, Stern Y (2015) The right insula contributes to memory awareness in cognitively diverse older adults. Neuropsychologia 75, 163–169. [PubMed: 26049091]

[65]. Leandrou S, Petroudi S, Kyriacou PA, Reyes-Aldasoro CC, Pattichis CS (2018) Quantitative MRI brain studies in mild cognitive impairment and Alzheimer's disease: A methodological review. IEEE Rev Biomed Eng 11, 97–111. [PubMed: 29994606]

[66]. Tabatabaei-Jafari H, Shaw ME, Cherbuin N (2015) Cerebral atrophy in mild cognitive impairment: A systematic review with meta-analysis. Alzheimers Dement (Amst) 1, 487–504. [PubMed: 27239527]

[67]. Liem F, Mérillat S, Bezzola L, Hirsiger S, Philipp M, Madhyastha T, Jäncke L (2015) Reliability and statistical power analysis of cortical and subcortical FreeSurfer metrics in a large sample of healthy elderly. Neuroimage 108, 95–109. [PubMed: 25534113]

[68]. Iscan Z, Jin TB, Kendrick A, Szeglin B, Lu H, Trivedi M, Fava M, McGrath PJ, Weissman M, Kurian BT (2015) Test–retest reliability of FreeSurfer measurements within and between sites: Effects of visual approval process. Hum Brain Mapp 36, 3472–3485. [PubMed: 26033168]

[69]. Seiger R, Ganger S, Kranz GS, Hahn A, Lanzenberger R (2018) Cortical thickness estimations ofFreeSurfer and the CAT12 toolbox in patients with Alzheimer's disease and healthy controls. J Neuroimaging 28, 515–523. [PubMed: 29766613]

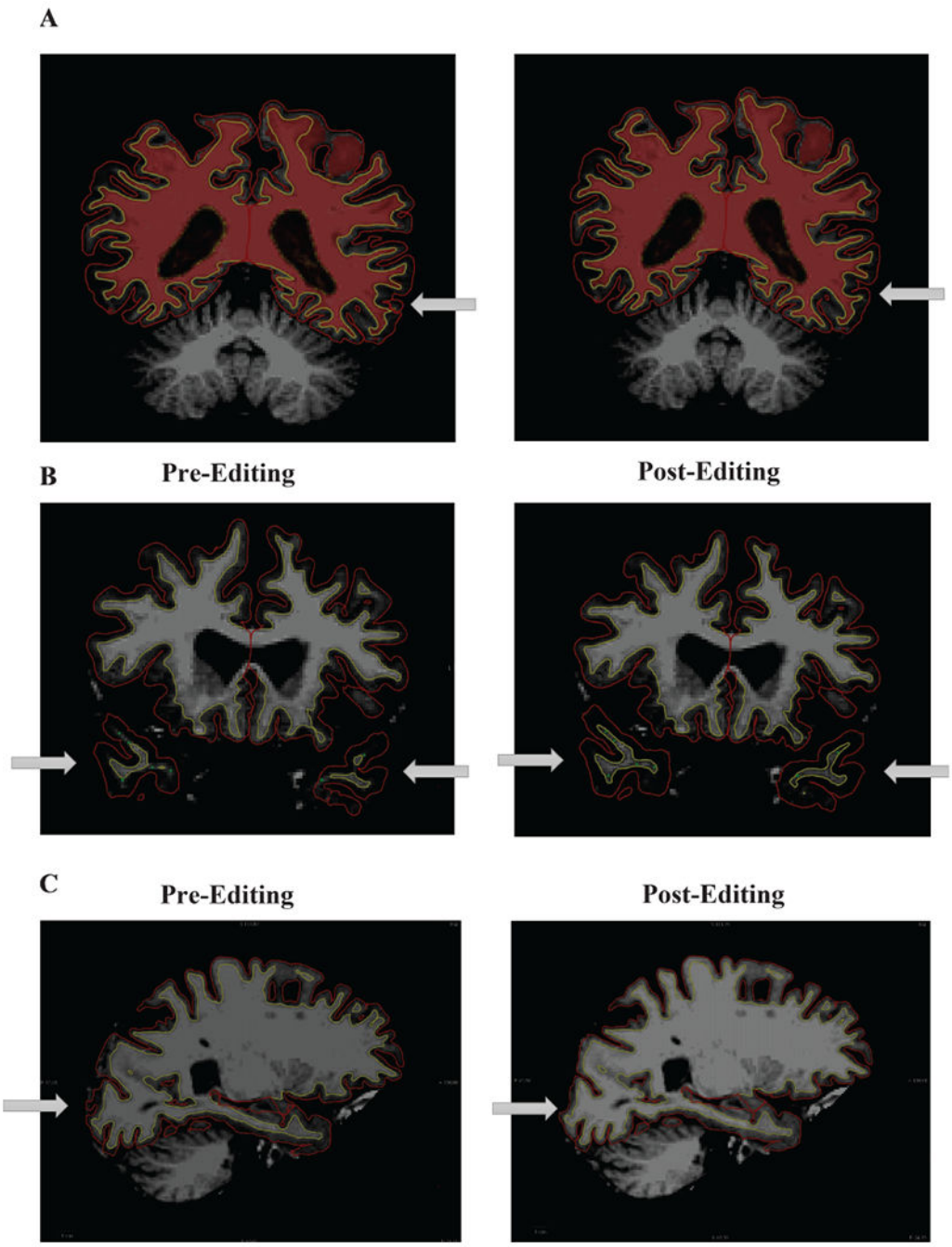

Fig. 1.

Examples of cortical error corrections made following FreeSurfer Version 6.0 processing. Panel A shows a topographical error that was corrected by adding white matter voxels. Panel B shows intensity bias errors that were corrected by adding control points. Panel C shows a pial displacement that was corrected by removing voxels.

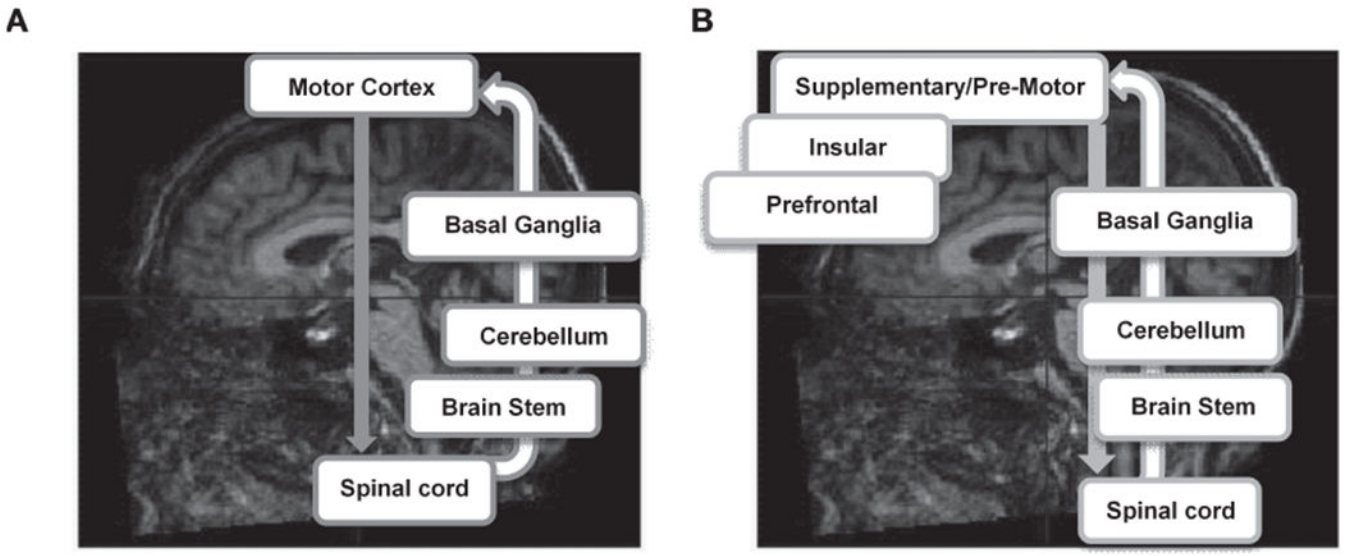

Fig. 2.
Abbreviated schematic of the motoric (A) and the control (B) pathway of human locomotion.

Table 1

Demographic characteristics as a function of MCR status in the whole sample, and as a function of study site

	MCR (All cohorts)	Non-MCR (All cohorts)	MCR (CCMA)	Non-MCR (CCMA)	MCR (TASCOG)	Non-MCR (TASCOG)	MCR (GAIT)	Non-MCR (GAIT)	MCR (NCGG-SGS)	Non-MCR MCR (NCGG-SGS)
N	66	133	7	42	9	41	25	25	25	25
Age in years; *M* (*SD*)	70.74 (6.46)	73.5 (4.08)	74.69 (4.51)	73.97 (1.91)	77.45 (10.37)	78.27 (0.92)	71.01 (4.42)	71.01 (1.40)	66.96 (4.03)	67.64 (0.49)
Sex; % female (N)	45 (30)	49 (65)	57 (4)	52 (22)	0.53 (5)	56 (23)	32 (8)	32 (8)	52 (13)	48 (12)
Education										
5–8 y; %(N)	27 (18)	14 (19)	14 (1)	0 (0)	67 (6)	32 (13)	44 (11)	24 (6)	0 (0)	0 (0)
9–12 y; %(N)	51 (34)	37 (49)	29 (20)	17 (7)	22 (2)	44 (18)	40 (10)	28 (7)	80 (20)	68 (17)
≥13 y;%(N)	21 (14)	49 (65)	57 (4)	83(35)	11 (1)	24 (10)	4	48 (12)	20 (5)	32 (8)
Mild cognitive impairment; %(N)	36 (24)	0 (0)	43 (3)	0 (0)	11 (1)	0 (0)	56 (14)	0 (0)	24 (6)	0 (0)
Total intracranial volume, mm^3; *M*	1,463,730	1,480,482	1,399,811	1,396,063	145,563	1,593,316	152,648	113,843	1,378,136	1,370,648
white matter lesion, mm^3; Mdn	2,663	2,538	2,853	2,322	6,861	4,238	2,626	1,613	2,035	2,232

Table 2

The effect of MCR on Cortical Measures in Multivariate and Follow-up Univariate General Linear Models, following no manual correction of the cortical surface and following manual correction of the cortical surface. All models were adjusted for age, sex, education, overall white matter lesion burden, total intracranial volume, and study site. The reliability of each model was estimated using 1,000 bootstrap samples (n-1; with resampling). **Bold numbers** indicate statistically significant results

	Original Estimate (Wilk's Lambda)	***p***				**"Corrected" Estimate (Wilk's Lambda)**	***p***			
Cortical Thickness: Multivariate GLM	**0.744**	**0.037**				**0.730**	**0.019**			
Cortical Thickness: Univariate GLMs	**Original Estimate (b)**	**95% CI (lower)**	**95% CI (upper)**	***p***	**FDR adjusted critical *p***	**"Corrected" Estimate (b)**	**95% CI (lower)**	**95% CI (upper)**	***p***	**FDR adjusted critical *p***
Bank of Superior Temporal Sulcus	−0.111	−0.252	0.029	0.120	0.040	−0.112	−0.243	0.019	0.093	0.034
Caudal Anterior Cingulate	−0.070	−0.218	0.078	0.353	0.047	−0.093	−0.271	0.086	0.309	0.047
Caudal Middle Frontal	−0.136	−0.253	−0.018	0.023	0.022	−0.135	−0.252	−0.018	0.024	0.022
Cuneus	−0.031	−0.141	0.079	0.576	0.049	−0.012	−0.119	0.097	0.835	0.050
Entorhinal	−0.307	−0.508	−0.107	**0.003**	**0.006**	−0.308	−0.510	−0.106	**0.003**	**0.007**
Fusiform	−0.150	−0.281	−0.020	0.024	0.024	−0.135	−0.252	−0.018	0.024	0.021
Inferior Parietal	−0.155	−0.258	−0.052	**0.003**	**0.004**	−0.153	−0.251	−0.055	**0.002**	**0.004**
Inferior Temporal	−0.119	−0.218	−0.019	0.020	0.019	−0.093	−0.188	0.002	0.054	0.031
Isthmus Cingulate	−0.144	−0.270	−0.018	**0.025**	**0.026**	−0.127	−0.249	−0.004	0.043	0.025
Lateral Occipital	−0.092	−0.188	0.003	0.057	0.032	−0.074	−0.166	0.017	0.111	0.040
Lateral Orbitofrontal	−0.152	−0.273	−0.031	**0.014**	**0.015**	−0.147	−0.262	−0.033	**0.011**	**0.012**
Lingual	−0.074	−0.121	0.003	0.060	0.034	−0.063	−0.138	0.012	0.097	0.037
Medial Orbitofrontal	−0.164	−0.286	−0.042	**0.009**	**0.010**	−0.189	−0.312	−0.067	**0.002**	**0.006**
Middle Temporal	−0.095	−0.214	0.024	0.118	0.038	−0.097	−0.211	0.017	0.096	0.035
Parahippocampal	−0.045	−0.230	0.140	0.633	0.050	0.034	−0.215	0.147	0.713	0.049
Paracentral	−0.180	−0.313	−0.047	0.008	0.007	−0.170	−0.299	−0.042	0.009	0.009
Parsopercularis	−0.077	−0.178	0.024	0.137	0.041	−0.072	−0.173	0.028	0.160	0.044
Parsorbitalis	−0.174	−0.305	−0.043	**0.009**	**0.012**	−0.158	−0.289	−0.028	0.018	0.016

	Original Estimate (Wilk's Lambda)	*p*				"Corrected" Estimate (Wilk's Lambda)	*p*			
Cortical Thickness: Multivariate GLM	**0.744**	**0.037**				**0.730**	**0.019**			
Cortical Thickness: Univariate GLMs	**Original Estimate (b)**	**95% CI (lower)**	**95% CI (upper)**	***p***	**FDR adjusted critical *p***	**"Corrected" Estimate (b)**	**95% CI (lower)**	**95% CI (upper)**	***p***	**FDR adjusted critical *p***
Parstriangularis	−0.198	−0.284	−0.113	**0.000**	**0.001**	−0.180	−0.272	−0.089	**0.000**	**0.001**
Pericalcarine	−0.077	−0.149	−0.004	0.039	0.029	−0.078	−0.154	−0.002	0.044	0.028
Postcentral	−0.055	−0.144	0.033	0.223	0.046	−0.069	−0.156	0.018	0.118	0.041
Posterior Cingulate	−0.153	−0.275	−0.031	**0.014**	**0.016**	−0.142	−0.261	−0.023	0.019	0.018
Precentral	−0.169	−0.304	−0.035	0.014	0.013	−0.166	−0.298	−0.033	0.014	0.013
Precuneus	−0.122	−0.229	−0.015	0.025	0.025	−0.116	−0.218	−0.013	0.027	0.024
Rostral Anterior Cingulate	−0.154	−0.320	0.012	0.070	0.037	−0.132	−0.306	0.042	0.138	0.043
Rostral Middle Frontal	−0.097	−0.193	−0.001	0.047	0.031	−0.086	−0.188	0.016	0.099	0.038
Superior Frontal	−0.124	−0.238	−0.010	0.034	0.028	−0.116	−0.233	0.002	0.053	0.029
Superior Parietal	−0.075	−0.187	0.036	0.186	0.044	−0.068	−0.173	0.037	0.203	0.046
Superior Temporal	−0.123	−0.222	−0.024	**0.015**	**0.018**	−0.125	−0.225	−0.025	0.015	0.015
Supramarginal	−0.129	−0.226	−0.033	0.009	0.009	−0.127	−0.224	−0.031	**0.010**	**0.010**
Frontal Pole	−0.153	−0.359	0.053	0.145	0.043	−0.202	−0.414	0.011	0.063	0.032
Temporal Pole	−0.250	−0.463	−0.037	0.021	0.021	−0.244	−0.449	−0.037	0.021	0.019
Transverse Temporal	−0.135	−0.277	0.007	0.063	0.035	−0.139	−0.274	−0.004	0.043	0.026
Insula	−0.177	−0.291	−0.065	**0.002**	**0.003**	−0.173	−0.278	−0.068	**0.001**	**0.003**
	Original Estimate (Wilk's Lambda)	***p***				**"Corrected" Estimate (Wilk's Lambda)**	***p***			
Cortical Volume: Multivariate GLM	**0.751**	**0.051**				**0.763**	**0.084**			
Cortical Volume: Univariate GLMs	**Original Estimate (b)**	**95% CI (lower)**	**95% CI (upper)**	***p***	**FDR adjusted critical *p***	**"Corrected" Estimate (b)**	**95% CI (lower)**	**95% CI (upper)**	***p***	**FDR adjusted critical *p***

	Original Estimate (Wilk's Lambda)	*p*				"Corrected" Estimate (Wilk's Lambda)	*p*			
Cortical Thickness: Multivariate GLM	**0.744**	**0.037**				**0.730**	**0.019**			
Cortical Thickness: Univariate GLMs	**Original Estimate (b)**	**95% CI (lower)**	**95% CI (upper)**	***p***	**FDR adjusted critical *p***	**"Corrected" Estimate (b)**	**95% CI (lower)**	**95% CI (upper)**	***p***	**FDR adjusted critical *p***
Bank of Superior Temporal Sulcus	−172.26	−354.483	9.962	0.064	0.021	−182.685	−368.130	2.761	0.054	0.018
Caudal Anterior Cingulate	−198.221	−403.086	6.644	0.058	0.019	−260.373	−455.754	−64.992	0.009	0.003
Caudal Middle Frontal	−158.113	−1006.114	−156.111	0.007	0.003	−521.202	−916.086	−126.318	0.010	0.004
Cuneus	−85.271	−359.024	188.481	0.542	0.041	−34.461	−311.575	242.653	0.807	0.046
Entorhinal	−143.569	−363.286	76.148	0.200	0.034	−42.555	−265.217	180.107	0.708	0.044
Fusiform	−327.594	−990.361	335.173	0.333	0.038	−272.945	−891.281	345.391	0.387	0.038
Inferior Parietal	−1437.700	−2316.881	−2316.881	**0.001**	**0.001**	−1336.273	−2166.506	−506.039	0.002	0.001
Inferior Temporal	−144.318	−867.744	579.108	0.696	0.046	−82.722	−780.429	614.985	0.816	0.047
Isthmus Cingulate	−241.084	−433.850	−48.317	0.014	0.009	−180.067	−368.716	8.583	0.061	0.019
Lateral Occipital	−169.806	−1070.062	730.451	0.712	0.047	−27.697	−861.951	806.556	0.948	0.050
Lateral Orbitofrontal	−388.579	−749.005	−28.155	0.035	0.015	−288.918	−602.189	24.353	0.071	0.022
Lingual	−441.777	−964.122	80.568	0.097	0.026	−361.867	−854.059	130.325	0.150	0.029
Medial Orbitofrontal	−261.957	−552.884	28.971	0.078	0.024	−311.952	−573.884	−50.020	0.020	0.010
Middle Temporal	−54.925	−746.336	636.485	0.876	0.049	−137.003	−804.555	530.549	0.688	0.043
Parahippocampal	−39.472	−206.044	127.100	0.642	0.044	−52.074	−225.749	121.601	0.557	0.041
Paracentral	−266.819	−513.218	−20.421	0.034	0.013	−223.823	−459.318	11.672	0.062	0.021
Parsopercularis	−180.149	−483.739	123.440	0.245	0.035	−156.306	−451.619	139.009	0.300	0.035
Parsorbitalis	−12.358	−188.557	163.840	0.891	0.050	15.0403	−152.171	182.251	0.860	0.049
Parstriangularis	−203.276	−464.987	58.436	0.128	0.029	−220.743	−483.519	42.034	0.100	0.026
Pericalcarine	−208.4935	−448.142	31.155	0.088	0.025	−186.549	−434.495	613.972	0.140	0.028
Postcentral	−181.396	−694.555	331.763	0.488	0.040	−187.756	−688.177	312.666	0.462	0.040
Posterior Cingulate	−299.6317	−544.889	−54.374	0.017	0.010	−302.851	−561.711	−43.992	0.022	0.013
Precentral	−652.2018	−1438.266	133.862	0.104	0.028	−538.900	−1296.096	218.296	0.163	0.031
Precuneus	−772.908	−1358.380	−187.433	0.010	0.006	−622.170	−1186.090	−58.249	0.031	0.016

	Original Estimate (Wilk's Lambda)	*p*				"Corrected" Estimate (Wilk's Lambda)	*p*			
Cortical Thickness: Multivariate GLM	**0.744**	**0.037**				**0.730**	**0.019**			
Cortical Thickness: Univariate GLMs	**Original Estimate (b)**	**95% CI (lower)**	**95% CI (upper)**	***p***	**FDR adjusted critical *p***	**"Corrected" Estimate (b)**	**95% CI (lower)**	**95% CI (upper)**	***p***	**FDR adjusted critical *p***
Rostral Anterior Cingulate	−218.5518	−420.927	−16.176	0.034	0.012	−240.919	−439.567	−42.270	0.017	0.009
Rostral Middle Frontal	−1186.111	−2085.530	−286.691	0.010	0.007	−1076.639	−1981.118	−172.159	0.020	0.012
Superior Frontal	−1228.003	−237.322	−77.684	0.036	0.016	−1347.704	−2437.605	−257.804	0.015	0.007
Superior Parietal	−1084.397	−1900.742	−268.052	0.009	0.004	−842.923	−1600.443	−85.402	0.029	0.015
Superior Temporal	−459.451	−1109.842	190.940	0.166	0.032	−533.024	−1163.227	97.179	0.097	0.025
Supramarginal	−415.352	−1139.585	308.882	0.261	0.037	−377.111	−1091.818	337.596	0.301	0.037
Frontal Pole	−36.738	−156.034	82.558	0.546	0.043	−52.959	−152.794	46.875	0.298	0.032
Temporal Pole	−192.359	−401.606	16.887	0.072	0.022	−115.1445	−332.820	102.531	0.300	0.034
Transverse Temporal	−91.463	−177.389	−5.538	0.037	0.018	−105.651	−188.557	−22.745	0.013	0.006
Insula	−267.062	−642.740	108.616	0.164	0.031	−307.125	−662.007	47.757	0.090	0.024
	Original Estimate (Wilk's Lambda)	***p***				**"Corrected" Estimate (Wilk's Lambda)**	***p***			
Cortical Surface Area: Multivariate GLM	**0.774**	**0.130**				**0.756**	**0.066**			
Cortical Surface Area: Univariate GLMs	**Original Estimate (b)**	**95% CI (lower)**	**95% CI (upper)**	***p***	**FDR adjusted critical *p***	**"Corrected" Estimate (b)**	**95% CI (lower)**	**95% CI (upper)**	***p***	**FDR adjusted critical *p***
Bank of Superior Temporal Sulcus	−6.025	−67.207	55.157	0.847	0.046	−8.447	−76.127	59.233	0.807	0.004
Caudal Anterior Cingulate	−13.493	−85.703	58.718	0.714	0.038	−45.040	−104.133	14.052	0.135	0.026
Caudal Middle Frontal	−86.658	−271.414	98.097	0.358	0.015	−53.350	−227.311	120.609	0.548	0.050
Cuneus	0.219	−119.469	119.907	0.997	0.050	1.723	−118.005	121.451	0.977	0.010
Entorhinal	14.646	−29.843	59.135	0.519	0.028	28.911	−19.138	76.959	0.238	0.024
Fusiform	76.802	−86.192	239.795	0.356	0.013	58.438	−119.762	236.637	0.520	0.007

	Original Estimate (Wilk's Lambda)	*p*				"Corrected" Estimate (Wilk's Lambda)	*p*			
Cortical Thickness: Multivariate GLM	**0.744**	**0.037**				**0.730**	**0.019**			
Cortical Thickness: Univariate GLMs	**Original Estimate (b)**	**95% CI (lower)**	**95% CI (upper)**	***p***	**FDR adjusted critical *p***	**"Corrected" Estimate (b)**	**95% CI (lower)**	**95% CI (upper)**	***p***	**FDR adjusted critical *p***
Inferior Parietal	−243.935	−553.245	65.375	0.122	0.003	−204.654	−516.691	107.383	0.199	0.037
Inferior Temporal	90.904	−132.953	314.760	0.426	0.019	50.947	−160.237	262.132	0.636	0.047
Isthmus Cingulate	−21.379	−93.099	50.341	0.559	0.032	−3.362	−70.524	63.801	0.922	0.013
Lateral Occipital	155.746	−168.069	479.561	0.346	0.012	160.019	−148.771	468.809	0.310	0.043
Lateral Orbitofrontal	1.139	−174.627	176.906	0.990	0.049	16.846	−137.429	171.122	0.831	0.029
Lingual	−81.064	−312.187	150.059	0.492	0.024	−66.939	−300.704	166.826	0.575	0.003
Medial Orbitofrontal	65.983	−51.368	183.333	0.270	0.006	85.745	−24.615	196.105	0.128	0.034
Middle Temporal	−730.285	−2393.523	932.954	0.389	0.018	54.572	−150.729	259.874	0.602	0.022
Parahippocampal	−6.393	−40.228	27.442	0.711	0.037	−11.513	−46.407	23.382	0.518	0.019
Paracentral	23.619	52.744	99.981	0.554	0.031	36.082	−42.987	115.152	0.371	0.044
Parsopercularis	−14.274	−115.419	86.870	0.782	0.044	−8.859	−114.829	97.110	0.870	0.001
Parsorbitalis	49.867	2.691	97.403	0.039	0.001	50.372	4.151	96.593	0.033	0.025
Parstriangularis	46.414	−44.286	137.114	0.316	0.010	29.807	−63.171	122.784	0.530	0.035
Pericalcarine	−58.185	−212.847	96.477	0.461	0.022	−39.626	−199.671	120.419	0.627	0.012
Postcentral	78.861	126.272	283.994	0.451	0.021	103.706	−88.126	295.538	0.289	0.021
Posterior Cingulate	−30.564	−118.491	57.362	0.496	0.025	−36.859	−128.125	54.407	0.429	0.006
Precentral	125.727	−147.205	398.658	0.367	0.016	190.467	−76.402	457.337	0.162	0.049
Precuneus	−41.566	−274.010	190.879	0.726	0.041	4.292	−226.409	234.994	0.971	0.046
Rostral Anterior Cingulate	16.798	−57.538	91.134	0.658	0.035	−5.315	−85.816	75.186	0.897	0.015
Rostral Middle Frontal	−177.009	−506.474	152.455	0.292	0.007	−164.999	−491.971	161.973	0.323	0.038
Superior Frontal	3.891	−395.067	402.849	0.985	0.047	−73.377	−501.528	354.773	0.737	0.016
Superior Parietal	−229.559	−552.291	95.174	0.166	0.004	−152.679	−461.070	155.711	0.332	0.040
Superior Temporal	50.691	−147.662	249.044	0.616	0.034	26.559	−172.679	225.799	0.794	0.032
Supramarginal	48.503	−218.794	315.799	0.722	0.040	68.926	−188.226	326.079	0.599	0.009
Frontal Pole	5.309	−11.541	22.159	0.537	0.029	9.153	−5.959	24.266	0.235	0.031

	Original Estimate (Wilk's Lambda)	*p*				"Corrected" Estimate (Wilk's Lambda)	*p*			
Cortical Thickness: Multivariate GLM	**0.744**	**0.037**				**0.730**	**0.019**			
Cortical Thickness: Univariate GLMs	**Original Estimate (b)**	**95% CI (lower)**	**95% CI (upper)**	***p***	**FDR adjusted critical *p***	**"Corrected" Estimate (b)**	**95% CI (lower)**	**95% CI (upper)**	***p***	**FDR adjusted critical *p***
Temporal Pole	6.143	−28.552	40.838	0.729	0.043	8.562	−21.776	38.899	0.580	0.018
Transverse Temporal	−9.712	−38.356	18.931	0.506	0.026	−14.318	−43.462	14.826	0.336	0.028
Insula	65.805	−60.172	191.782	0.306	0.009	37.946	−93.029	168.921	0.570	0.041